Hindawi Publishing Corporation
Journal of Fuels
Volume 2014, Article ID 946485, 9 pages
http://dx.doi.org/10.1155/2014/946485

Research Article

Performance Evaluation of a Small-Scale Turbojet Engine Running on Palm Oil Biodiesel Blends

A. R. Abu Talib, E. Gires, and M. T. Ahmad

Propulsion and Thermofluid Research Group, Department of Aerospace Engineering, Faculty of Engineering, Universiti Putra Malaysia, Malaysia

Correspondence should be addressed to A. R. Abu Talib; abdrahim@upm.edu.my

Received 22 October 2013; Revised 2 May 2014; Accepted 3 May 2014; Published 8 July 2014

Academic Editor: Xingcai Lu

The experimental and simulated performance of an Armfield CM4 turbojet engine was investigated for palm oil methyl ester biodiesel (PME) and its blends with conventional Jet A-1 fuel. The volumetric blends of PME with Jet A-1 are 20, 50, 70, and 100% (B20, B50, B70, and B100). Fuel heating values (FHV) of each fuel mixture were obtained by calorimetric analysis. The experimental tests included performance tests for Jet A-1 and B20, while the performances of B50 to B100 were simulated using GasTurb 11 analytical software. In terms of maximum measured thrust, Jet A-1 yielded the highest value of 216 N, decreasing by 0.77%, 4%, 8%, and 12% with B20, B50, B70, and B100. It was found that B20 produced comparable results compared to the benchmark Jet A-1 tests, particularly with thrust and thermal efficiency. Slight performance penalties occurred due to the lower energy content of the biodiesel blends. The efficiency of the combustor improved with the addition of biodiesel while the other component efficiencies remained collectively consistent. This research shows that, at least for larger gas turbines, PME is suitable for use as an additive to Jet A-1 within 50% blends.

1. Introduction

There is a general consensus within the literature that fossil fuel feedstock used for the production of aviation-grade kerosene fuel is dwindling. Koh and Ghazoul [1] expected a peak oil production scenario within the years 2010–2020, assuming that global oil consumption increases to 118 million barrels per day in 2030. Nygren et al. [2] projected that civil aviation traffic growth will increase at a rate of 5% per year, while fuel consumption will increase at 3% per year. Lee et al. [3] projected that aviation traffic growth will increase by 4.5% to 6% per year over the next twenty years, with traffic doubling every 15 years. This is further supported by the recent report by Deloitte [4], whereby passenger travel demand is expected to increase 5% over the next 20 years, contributing to increases in aircraft production. Despite the improvements in aircraft fuel efficiency since 1960 [5], further efforts need to be made in order to mitigate the dependency on traditional fuel sources and to replace current petrol-based fuels.

Biodiesel is produced through the transesterification of pure vegetable or organic oils by replacing the triglyceride molecules with lighter alcohol molecules such as methanol or ethanol. The reaction is carried out with a strong base catalyst, producing glycerol in addition to transesterified vegetable oils (biodiesel) [6]. Canakci et al. [7] claimed that biodiesel CO_2 emissions are offset through photosynthesis. In addition to its carbon offset, biodiesel is nontoxic, contains no aromatics or sulfur, has higher biodegradability, and is less polluting to water and soil upon spillage, as opposed to kerosene [8]. In addition, biodiesels do not contain trace metals, carcinogens like polyaromatic hydrocarbons, and other pollutants that are directly detrimental to human health [9]. Significant reduction of emissions particulate was reported by Chan et. al [10] when they used a blend of 50% volume of camelina-based hydro-processed biojet fuel with F-34 jet fuel in a T-56 turbo-prop engine.

In the short and medium term, palm oil biodiesel (PME) may be utilized as a prime source for biodiesel production. According to Sumathi et al. [11], oil palm cultivation and processing require little input of agrochemical fertilizers and fossil fuels to produce 1 ton of oil. From 2007 data collected by Sumathi et al. [11], the oil yield from oil palm

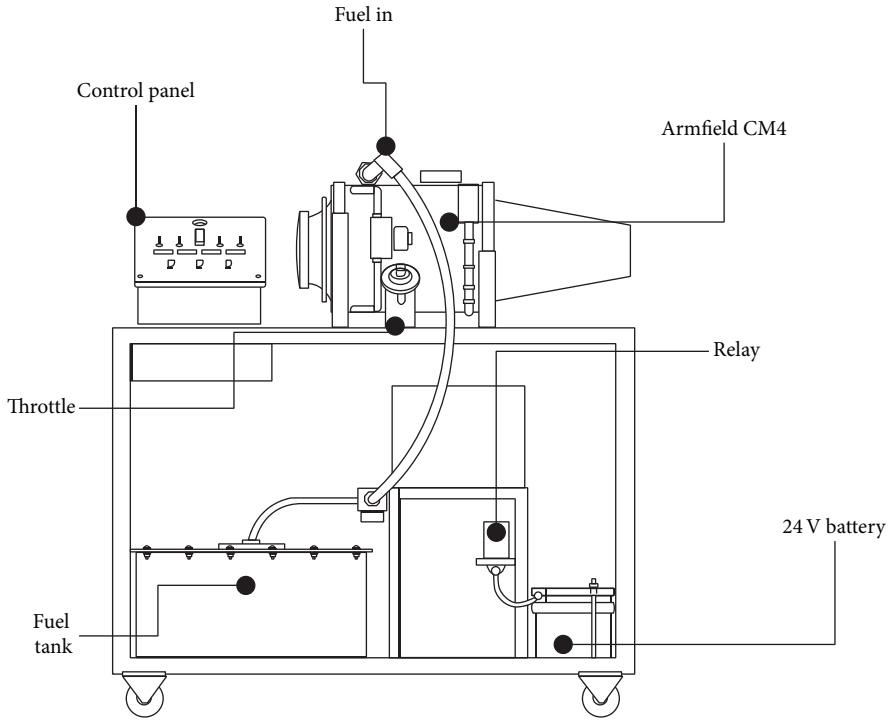

Figure 1: Armfield CM4 turbojet engine.

was 3.74 ton/hectare/year, which is 10 times more than soybean during the same period (0.38 ton/hectare/year). This makes oil palm currently the highest yielding oil crop in the world [11], and, hence, an attractive biodiesel substitute or supplement to aviation kerosene. This is supported by the work done by Chong and Hochgreb [12] that reported that the NO_x emissions per unit energy are reduced by using PME compared to diesel and Jet A.

French [13] tested the performance of a turbine technologies SR-30 turbojet gas turbine engine using canola oil biodiesel. It was found that the maximum thrust achieved by the biodiesel was less than Jet-A by 8% at maximum rpm. Using a gas turbine engine of the same model as French [13], Habib et al. [14] tested a variety of biodiesels and biofuels in 50% and 100% (B50, B100) volumetric blends with Jet A-1. In terms of thrust specific fuel consumption (TSFC), at higher rpm, the TSFC of all test fuels was not significantly different from that of Jet A-1. The turbine inlet temperature (TIT) for biofuels was higher than that of Jet A-1 overall. The exhaust gas temperature (EGT) was similar for all test fuels.

Chiang et al. [15] tested a 150 kW Teledyne RGT-3600 micro gas turbine running on an unspecified biodiesel in volumetric blends of 10%, 20%, and 30% with diesel. All of the biodiesel blends had similar thermal efficiencies across all power loads. It was reported that carbon deposits were found after operating for 6 hours on biodiesel blends on the fuel nozzle [15]. Krishna [16] tested soy biodiesel (SME) in volumetric blends of 20%, 50%, and 100% (B20, B50, and B100) with ASTM number 2 heating oil in a 30 kW capstone CR30 gas fired microturbine. It was found that the heating efficiencies of number 2 heating oil, B20, and B100 were similar, at approximately 20%. B50 heating efficiency was higher by 7%.

A consensus between most of the related works is that smaller quantities of biodiesel blended with the benchmark fuel, be it diesel or aviation kerosene fuels, did not adversely affect the performance capabilities of the test engines. In this study, palm oil biodiesel is tested in 20% volume with Jet A-1 in order to verify the findings of other gas turbine research tests on biofuel blends. In addition, higher concentrations of PME in Jet A-1 blends were tested in simulations of the CM4 engine.

2. Description of Apparatus

In order to provide a functional turbojet engine for educational and research purposes, Armfield modified the allied signal JFS100-13A into the CM4 turbojet engine. A schematic of the engine is shown in Figure 1. The CM4 turbojet engine can be broken down into five distinct main components: (i) inlet; (ii) centrifugal compressor; (iii) combustor (burner); (iv) axial turbine; and (v) exhaust nozzle. The above components are simplified in Figure 2. The manufacturer specifications for the JFS100 and, by extension, the CM4 are summarized in Table 1. Table 2 shows the range of sensors that came equipped with the CM4 turbojet as well as the properties measured.

2.1. Preparation of Test Fuels. Palm oil biodiesel is a fatty acid methyl ester that is amber in color and is noticeably viscous in comparison to Jet A-1 fuel, which is straw and less opaque in color. The Jet A-1 fuel used in this research project

Table 1: Manufacturer and original equipment specifications.

Model and type	JFS100-13A
Compressor	Air inlet in front of unit Single stage radial outflow
Air mass flow	0.726 kg/s at 72500 rpm
Compression ratio	3.5 : 1
Combustor	Annular fuel manifold assembly Five simplex fuel nozzles
Turbine	1-stage axial flow turbine Maximum temperature 1000°C
Width and height	302.26 mm and 304.80 mm
Length	558.80 mm
Weight	37.195 kg dry 38.102 kg with lubricant
Fuel	K-1 kerosene or Jet-A
Power rating	67.11 kW at 60400 rpm
Maximum thrust	300 to 400 N optimal
CM4 optimal shaft speed	70000 rpm
CM4 exhaust gas temperature	Maximum 800°C

Table 2: CM4 sensors and placements.

Location	Sensor type	Measured parameters
Inlet	Type K Thermocouple	Inlet temperature T_1
Compressor	Type K Thermocouple	Entry temperature T_1
	Pitot tube	Entry pressure P_1
	Type K Thermocouple	Exit temperature T_2
	Pitot tube	Exit pressure $P_2 = P_3$
Turbine	Type K Thermocouple	Entry temperature T_3
	Type K Thermocouple	Exit temperature T_4
	Pitot tube	Exit pressure P_4
Nozzle	Type K Thermocouple	Exit temperature $T_5 = T_4$
	Pitot tube	Exit pressure P_5
Starter gear	Magnetic pickup optical sensor (0–100000 rpm)	Shaft speed
Between front of engine and frame of test rig	Load cell	Thrust F

was obtained from Petronas Malaysia, whereas Sime Darby supplied the PME fuel. It was found that PME mixes readily with Jet A-1. Each volume of fuel was mixed in a glass beaker with the aid of a glass-stirring rod. The mixtures were found to retain their structure and no separation was visible. This remained true for the entire duration of the research project for samples that were kept for several months. Furthermore,

Table 3: Fuel heating values for Jet A-1 and PME blends.

Fuel	Jet A-1	B20	B50	B70	B100
Fuel heating value (MJ/kg)	46.190	44.905	42.824	41.548	39.964

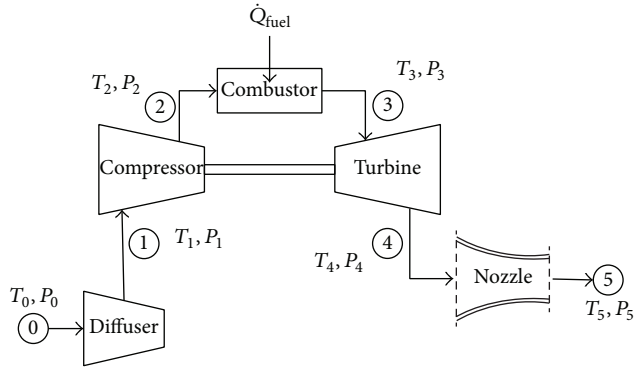

Figure 2: Schematic layout of engine components.

Figure 3: Test fuel samples; from left to right: Jet A-1, B20, B50, B70, and B100.

there was no visible water retained in the fuel blends. Figure 3 shows samples of the test fuels in increasing PME content.

Each fuel was also tested for its fuel heating or calorific values (FHV). This was done using an IKA C200 oxygen bomb calorimeter with the cooperation of the Faculty of Science and the technology of Universiti Kebangsaan Malaysia (UKM). Each test was performed three times to obtain a mean FHV for each fuel. Table 3 shows the range of FHV for the test fuels.

3. Experimental Procedure

All of the Armfield CM4 tests were conducted in the Propulsion Laboratory at the Faculty of Engineering, Universiti Putra Malaysia. In all cases, the larger shutter doors of the laboratory were opened such that the engine's exhaust would travel outwards of the laboratory. The tests conducted for the CM4 engine were all cold starts. This means that no fuel switching occurred during operation. Similar to the experiments of French [13] and Krishna [16], no modification to the internal turbomachinery of the test engine was made.

Upon ignition, the engine was given approximately one minute to reach a steady state whereby the engine speed remained constant at a minimum of 48000 rpm. The throttle was slowly raised from 48000 rpm to approximately 66000 rpm. At each 1000 rpm interval, a sampling period of 10 seconds was allowed to ensure more reliable average readings for each sensor. Once the maximum rpm was achieved and the relevant data was measured, the throttle was slowly closed in a similar, decremental fashion back to 48000 rpm. Sampling was then halted once the minimum rpm was achieved. Tests for Jet A-1 and B20 were repeated at least three times each.

The Armfield CM4 is equipped with a PC interface for its various sensors. The values of temperature, pressure, engine speed, and measured thrust are displayed in the user interface. An automatic sampling rate of every two seconds was set. Because of sensor limitations, the burner inlet and exit gauge pressures P_2 and P_3 were assumed to be equal, as were the turbine exit and nozzle exit temperatures T_4 and T_5.

3.1. Jet Engine Cycle Analysis. The basis of the calculation of performance parameters is the cycle analysis of gas turbines as demonstrated by Mattingly [17]. The primary measure of a turbojet engine is its thrust F, which is represented by

$$F = \dot{m}_5 V_5 - \dot{m}_0 V_0 + A_5 \left(P_{t5} - P_0\right), \tag{1}$$

where $\dot{m}_5$ is the total mass flow exiting the exhaust nozzle, V_5 is the nozzle exit velocity, $\dot{m}_0$ is the airflow ahead of the engine inlet, V_0 is the free stream air velocity, and the term $A_5(P_{t5} - P_0)$ refers to the thrust contribution from the pressure difference at the nozzle exit. The next performance parameters for the turbojet engine to be calculated are the specific thrust $F/\dot{m}_0$, fuel-air ratio f, and thrust specific fuel consumption S. Equation (2) show the equations used to obtain the aforementioned parameters. The FHV is represented as constant h_{PR}:

$$\begin{aligned} \frac{F}{\dot{m}_0} &= a_0 \cdot \frac{\dot{m}_5}{\dot{m}_0}\left(\frac{V_5}{a_0} - M_0\right) + \frac{A_5 P_5}{\dot{m}_0}\left(1 - \frac{P_0}{P_5}\right), \\ f &= \frac{1}{h_{PR}}\left(c_{p3} \cdot T_3 - c_{p2} \cdot T_2\right), \\ S &= \frac{f}{F/\dot{m}_0}. \end{aligned} \tag{2}$$

Following the above calculations, the engine thermal, propulsive, and overall efficiencies η_T, η_P, and η_O are obtained as shown in

$$\begin{aligned} \eta_T &= \frac{a_0^2 \cdot (1+f)\left[\left(V_5/a_0\right)^2 - M_0^2\right]}{2 \cdot f \cdot h_{PR}}, \\ \eta_P &= \frac{2V_0\left(F/\dot{m}_0\right)}{a_0^2\left[(1+f)\left(V_5/a_0\right)^2 - M_0^2\right]}, \\ \eta_O &= \eta_T \times \eta_P. \end{aligned} \tag{3}$$

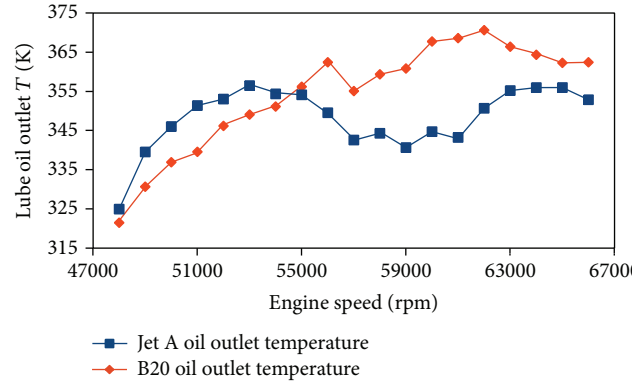

Figure 4: Lubrication oil temperatures for B20 and Jet A-1.

For the burner section, burner efficiency η_b is obtained from

$$\eta_b = \left(\tau_b \cdot f + \tau_b - 1\right) \times \frac{c_{p2} T_2}{h_{PR} f}, \tag{4}$$

where the term τ_b refers to the ratio of burner exit and inlet temperatures T_4/T_3.

In order to normalize the results from the experiments due to the differing ambient temperature T_0, corrections to the performance parameters with respect to standard sea level conditions were made. These corrections are listed below from (5). The remaining performance parameters were then calculated as previously based on the corrected values. The dimensionless variables δ_n and θ_n refer to the station pressure or temperature ratios in relation to standard sea level pressure and temperature 101.3 kPa and 288.2 K:

$$\begin{aligned} F_c &= \frac{F}{\delta_0}, \\ \dot{m}_{c0} &= \frac{\dot{m}_0}{\sqrt{\theta_0}/\delta_0}, \\ \dot{m}_{cf} &= \frac{\dot{m}_f}{\delta_1 \cdot \sqrt{\theta_1}}, \\ S_c &= \frac{\sqcap_d \cdot \dot{m}_{cf}}{F_c}. \end{aligned} \tag{5}$$

4. Experimental Results

As stated prior, the fuels that were tested experimentally were Jet A-1 and B20. Because the only factor taken into account is that the directly affected thrust is the throttle, most of the results are shown against the engine speed or rpm. Figure 4 shows the changes that occurred in the lubrication oil temperature for both fuels. The lubrication oil outlet temperature for B20 is clearly higher than that of Jet A-1, from 55000 rpm onwards. The largest rise in lubrication oil temperature is from 343.2 K to 368.6 K at 61000 rpm, an increase of 7.4%. This would imply that more stress is placed on the turbomachinery when using B20 fuel. The higher lubrication oil temperatures may also be attributed to the

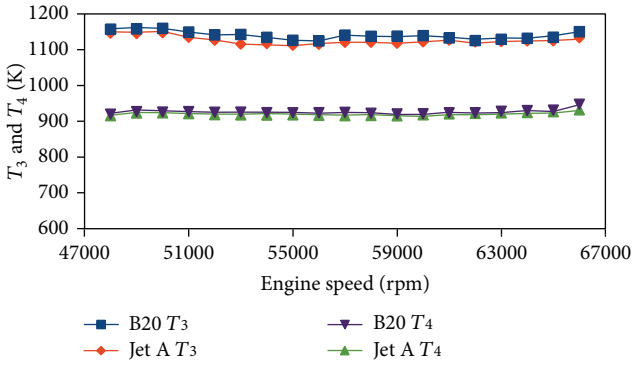

Figure 5: Turbine inlet and exit temperatures for B20, Jet A-1.

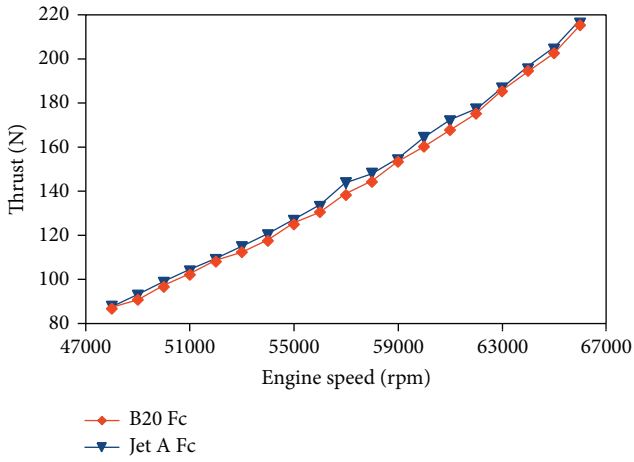

Figure 6: Corrected thrust lines for B20 and Jet A-1.

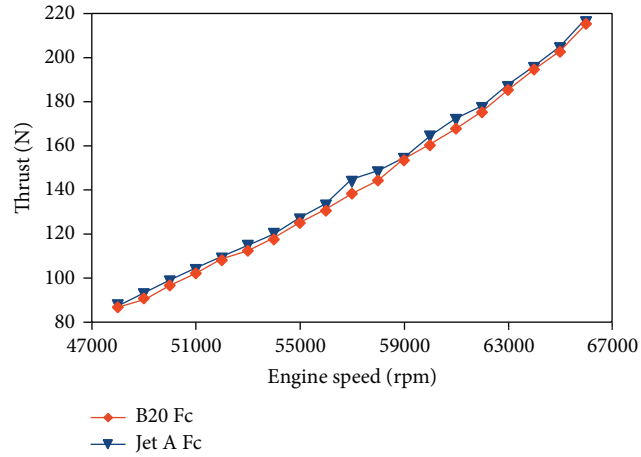

Figure 7: Corrected fuel flow rate for B20 and Jet A-1.

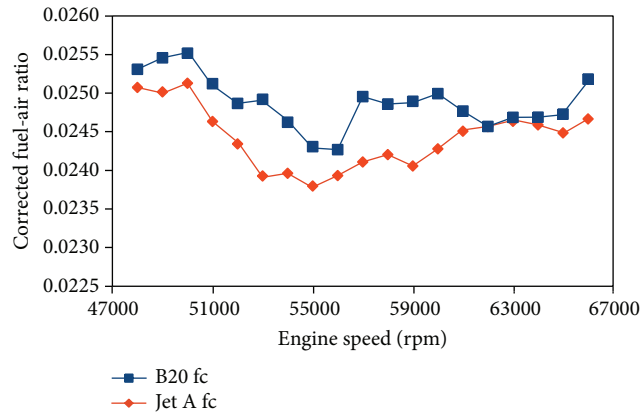

Figure 8: Fuel-air ratio for B20 and Jet A-1 fuels.

higher turbine temperatures during the B20 tests, shown in Figure 5.

The change in thrust for B20 from Jet A-1 is shown in Figure 6. It can be seen that in barring a 2% to 4% drop in thrust at the midrange of engine speed, B20 performs comparably with Jet A-1, to the point that, from 61000 rpm onwards, the difference in thrust is less than 1.5%.

Figures 6, 7, 8, and 9 show an interesting trend for the performance of the CM4 running on Jet A-1 and B20. The percentage differences between the two fuels' impact on thrust are very small, at most about 4%, with increasing similarity at the high rpm range. The findings tally with Krishna [16], whereby smaller quantities of biodiesel in the benchmark fuel did not lead to a significant drop in performance. The trend of converging parameters towards maximum rpm continues for air and fuel flow and thrust specific fuel consumption. This suggests that a 20% mixture of PME with Jet A-1 is viable, particularly at higher rpm. However, the CM4 still saw a small increase in fuel-air ratio and specific fuel consumption before reaching 60000 rpm. This can only be attributed to the slightly lower FHV of B20. This implies that slightly more B20 fuel is needed to achieve the same performance as that of Jet A-1.

As with the earlier performance indicators, B20 performed comparably to Jet A-1 for thermal efficiency (Figure 10); however, the differences in propulsive efficiency are clearer, with Jet A-1 having better propulsive efficiency at the higher engine speeds as shown in Figure 11. This leads to a similar percentage of difference for overall efficiency (Figure 12). The higher propulsive efficiency for Jet A-1 is due to its lower fuel-air ratio (Figure 8).

A more apparent change in component performance is seen in the burner section, which is made clearer in Figure 13. By burning B20, the combustor efficiency rose by approximately 2% on average. The higher burner efficiency is due to the completeness of the combustion process, which is due to the oxygen content of the biodiesel. This is also linked to the higher turbine temperatures mentioned prior.

5. GasTurb Analysis

Due to experimental constraints and concerns regarding fuel line integrity and ignition times for higher density blends of biodiesel, the performance of the Armfield CM4 using B50, B70, and B100 fuels was simulated to obtain performance trends after switching from Jet A-1. This was done by utilizing

Table 4: GasTurb input parameters for cycle analysis at 66000 rpm.

Input name as shown in GasTurb 11	Established reference variable	Value
Total temperature $T1$	T_0	300 K
Ambient pressure Pamb	P_0	101.1 kPa
Relative humidity		50% (based on average hygrometer readings in laboratory over test period)
Inlet Corr. Flow W2Rstd	$\dot{m}_0$	0.767 kg/s (from experimental results for Jet A-1)
Pressure ratio	π_c	2.63 (established from experimental results)
Burner exit temperature	T_3	1133.3 K (Jet A-1) 1150 K (B20)
Burner design efficiency	η_b	0.82
Fuel heating value	FHV or h_{PR}	46.190 MJ/kg (Jet A-1); dependent on test fuel. FHV obtained from Table 3
Mechanical efficiency	η_m	0.8815 (as iterated by GasTurb)
Compressor efficiency	η_c	0.77
Nominal spool speed		66000 rpm
Turbine efficiency	η_t	0.82

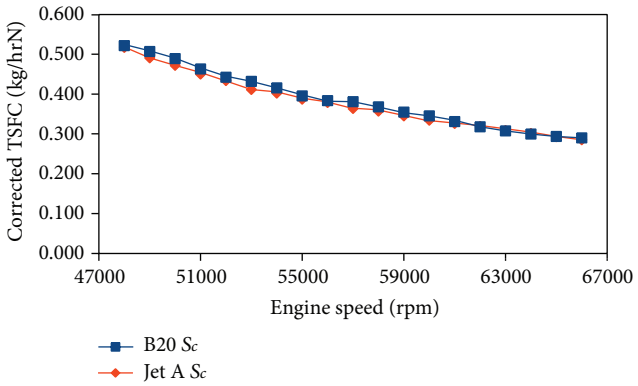

Figure 9: Corrected thrust specific fuel consumption for B20 and Jet A-1.

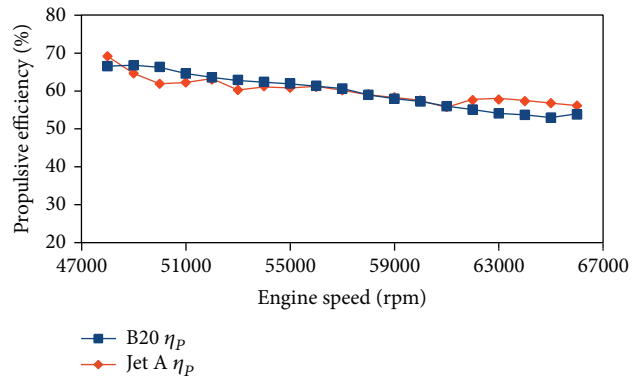

Figure 11: Propulsive efficiency for B20 and Jet A-1.

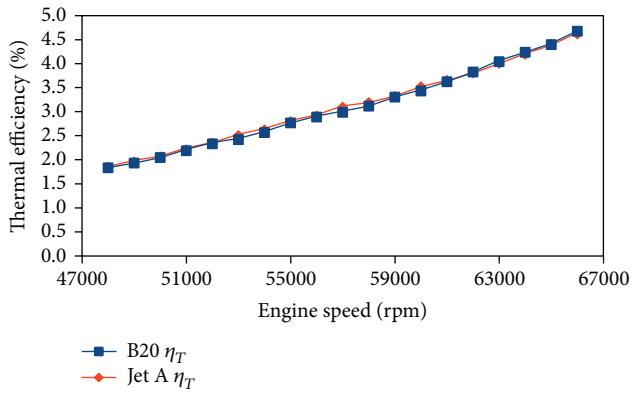

Figure 10: Thermal efficiency for B20 and Jet A-1.

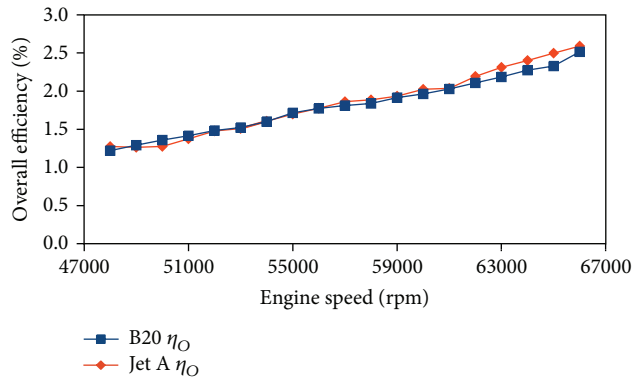

Figure 12: Overall efficiency for B20 and Jet A-1.

GasTurb 11, a gas turbine performance simulation program developed by Kurzke [18]. An earlier build of GasTurb was utilized by Habib et al. [14] when predicting the performance of 100% biodiesel after running experimental tests for 10, 20, and 30% biodiesel blends with petrodiesel. The list of GasTurb inputs used for the simulations for each test fuel is shown in Table 4, while Figure 14 shows the physical model of the simulated engine based on the specified inputs. Given

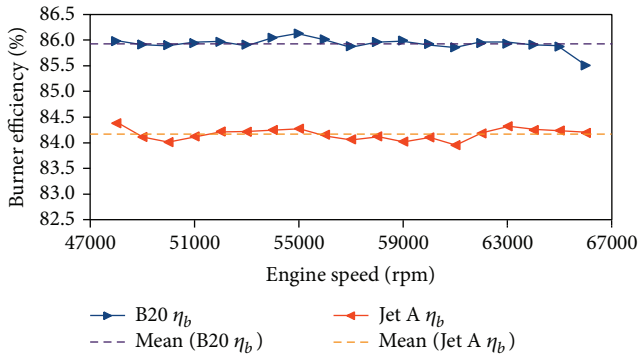

FIGURE 13: Burner efficiency for B20 and Jet A-1.

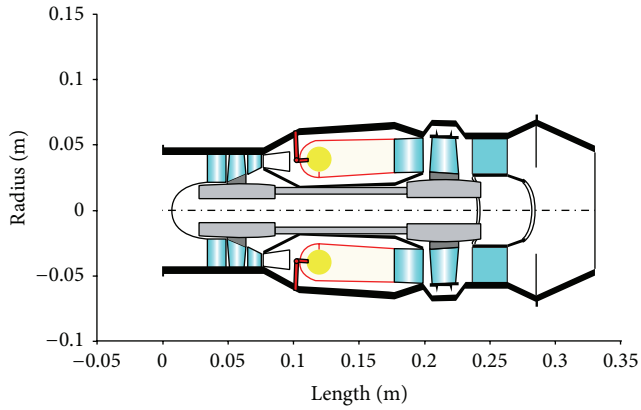

FIGURE 14: Engine model rendered by GasTurb 11.

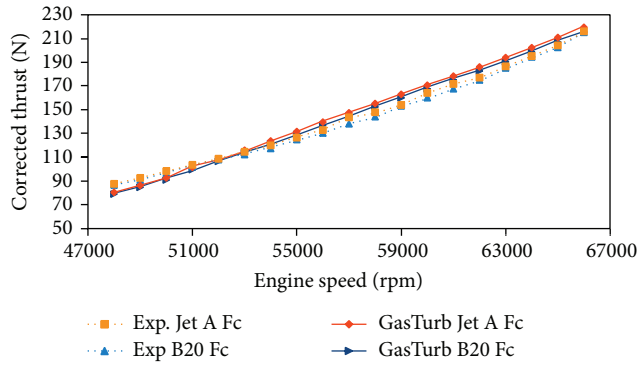

FIGURE 15: Simulation and experimental corrected thrust lines using Jet A-1 and B20 fuels.

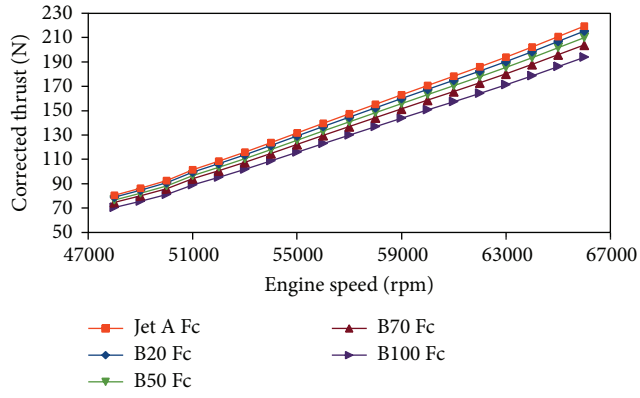

FIGURE 16: Simulation corrected thrust for all test fuels.

the small scale used by GasTurb it can be seen that the performance of the simulation is plausible for small engines such as the CM4.

Several assumptions and iterations had to be made in order to get as close an analogue to the actual CM4 engine as possible. Since the main performance data would involve thrust, the priority was to have a simulation with similar thrust output to the real CM4. The two thrust lines produced for Jet A-1 and B20 are shown in Figure 15 in comparison to their experimental counterparts. It is shown that the simulations are within good agreement with the experimental results for thrust. Figure 16 shows the corrected thrust lines for each simulated fuel from idle to maximum engine speed, while Figure 17 shows the TSFC trend for all fuels.

The thrust produced with increasing PME volume decreased from the Jet A-1 benchmark values across all engine speeds. The reduction in thrust became more pronounced with B70 and B100 fuels. In GasTurb, the maximum SSL corrected thrust from Jet A-1 was 219.4 N, which decreased to 215.4 N, 210.4 N, 203.7 N, and 194.1 N for B20, B50, B70, and B100. The biggest factor in the decrease of thrust was the reduction in FHV for each consecutive biodiesel blend. It is also shown that a straight 100% PME fuel is not desirable as maximum thrust is decreased by approximately 12%. The TSFC for each fuel showed that the S_c lines for Jet A-1, B20, and B50 were quite close to each other, with improved TSFC for B20 and B50 at the lower engine speeds and converging values with Jet A-1 towards maximum rpm, with slightly higher values at 66000 rpm. The increases in TSFC are much more pronounced for B70 and B100, with increases of 11% and 18% at maximum rpm.

The changes in thermal efficiency η_T for each test fuel at all engine speeds are shown in Figure 18. It can be seen that η_T is improved with the usage of B20 and B50 from idle rpm to approximately 63000 rpm, after which Jet A-1 has better η_T until maximum engine speed. The thermal efficiency deteriorated from Jet A-1 values under B100, dropping to 2.11% from the optimal Jet A-1 η_T, which was 2.45% at maximum rpm.

The results of the simulations for all test fuels at maximum rpm are shown in Table 5. The increase in specific fuel consumption for B100 is nearly 20% from that of Jet A-1. The overall efficiency of the engine decreased with increasing PME content. This is indicative of the lower FHV for the biofuels, leading to higher fuel flow and fuel consumption.

6. Conclusion and Recommendations

The aim of this experimental work was to determine the performance of the Armfield CM4 turbojet running on a spectrum of blends of palm oil biodiesel and Jet A-1. It was found that B20 produced similar amounts of thrust as Jet A-1,

Table 5: Optimal simulated jet cycle results for all test fuels at 66000 rpm.

Fuels at maximum rpm	Jet A-1	B20	B50	B70	B100
T_3 (K)	1133.30	1150.00	1161.00	1169.00	1180.00
T_4 (K)	945.80	960.42	968.73	973.93	981.57
F_c (N)	219.43	215.42	210.37	203.74	194.11
$\dot{m}_{cf}$ (kg s^{-1})	0.0140	0.0138	0.0141	0.0144	0.0147
$F_c/\dot{m}_{c0}$ (kg s^{-1})	280.12	285.04	282.17	277.08	271.27
f_c	0.0179	0.0183	0.0189	0.0196	0.0205
S_c (kg hrN^{-1})	0.2092	0.2101	0.2196	0.2314	0.2479
η_T (%)	2.45	2.47	2.42	2.29	2.11
η_O (%)	1.71	1.72	1.69	1.60	1.47

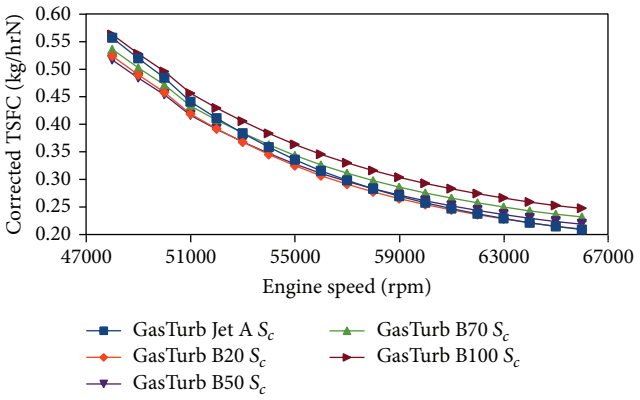

Figure 17: Simulation corrected TSFC for all test fuels.

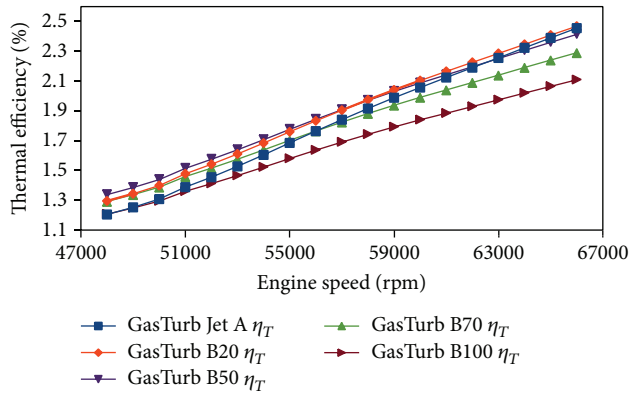

Figure 18: Simulation thermal efficiencies for all test fuels.

particularly at the higher range of rpm. The trade-offs from the usage of biodiesel include slightly higher fuel flow, fuel-air ratio, and specific fuel consumption, but from the B20 data the increase in these values was minimal, within a range of 0–5%. In addition, the thermal efficiency for B20 was of similar caliber to that of Jet A-1, while the propulsive and overall efficiencies underwent a slight drop at maximum rpm. The burner efficiency improved with the combustion of B20, due to its higher oxygen content.

With more concentrated blends of PME and Jet A-1, it was found that the net thrust produced decreased in larger degrees with increasing PME content. The thrust for Jet A-1, B20, and B50 was of comparable values, while B70 and B100 performed poorly in comparison. From the results, the threshold of volumetric content for PME before a noticeable drop in performance was found to be at 50%. It should also be noted that temperatures aft of the burner increased in proportion to increases in PME content.

The drawbacks for PME were higher turbine inlet and exit temperatures as well as its inherently lower calorific value. The long term effects of biodiesel testing in turbojet engines have not yet been studied, particularly in terms of combustor and turbine lining as well as fuel delivery systems. In addition, while B20 performed comparably well with Jet A-1, its lower FHV and higher viscosity need to be addressed to optimize the performance of the blend and to minimize deterioration of the fuel delivery systems.

In terms of the bigger picture of widespread usage in aero engines, while there have been instances of commercial flights using 50% blends of fatty acid methyl ester biodiesel with aviation kerosene, such a practice has not been formally institutionalized due to issues of economic and energy cost and availability of biodiesel in large quantities. However, as this research has shown, PME is a viable fuel for microturbine applications in both power generation and unmanned or remote controlled aerial vehicles.

Nomenclature

PME: Palm oil methyl ester biodiesel
XME: Methyl ester biodiesel of feedstock *X*
B*XX*: *XX*% volume of PME blended with Jet A-1
rpm: Engine speed (revolutions per minute)
h_{pr}: Fuel heating value (FHV)
0: Free stream subscript
c: Sea level value corrected subscript
T_n: Temperature at station *n*
P_n: Gauge pressure at station *n*
P_{tn}: Absolute pressure at station *n*
F: Net thrust
$\dot{m}_0$: Air mass flow rate
$\dot{m}_f$: Fuel flow rate
$\dot{m}_5$: Total mass flow rate
V_n: Velocity at station *n*
f: Fuel-air ratio

$F/\dot{m}_0$: Specific thrust
S: Thrust specific fuel consumption (TSFC)
a_n: Speed of sound at station n
M_n: Mach number at station n
c_{pn}: Specific heat capacity at station n
γ_n: Specific heat ratio at station n
τ: Temperature ratio between stations
π: Pressure ratio between stations
η: Efficiency
$w_{c,t}$: Specific work for compressor or turbine
$W_{c,t}$: Power produced by compressor or turbine
θ, δ: Sea level value temperature and pressure ratios.

Station Numbering and Subscripts

0: Free stream (upstream of engine inlet)
1: Inlet (d) of compressor
2: Compressor (c) exit or burner (b) inlet
3: Burner exit or turbine (t) inlet
4: Turbine exit or nozzle inlet
5: Nozzle exit.

Conflict of Interests

The authors declare that there is no conflict of interests regarding the publication of this paper.

Acknowledgments

This work was greatly supported by the Universiti Putra Malaysia (UPM), Research University Grant Scheme (RUGS) under the project no. 05-01-09-0719RU as well as the technical support staff at the Aerospace Engineering Department of UPM. Thanks are also extended to the Food Research Laboratory at Universiti Kebangsaan Malaysia (UKM) for providing the calorimetric testing of the test fuels.

References

[1] L. P. Koh and J. Ghazoul, "Biofuels, biodiversity, and people: understanding the conflicts and finding opportunities," *Biological Conservation*, vol. 141, no. 10, pp. 2450–2460, 2008.

[2] E. Nygren, K. Aleklett, and M. Höök, "Aviation fuel and future oil production scenarios," *Energy Policy*, vol. 37, no. 10, pp. 4003–4010, 2009.

[3] D. S. Lee, D. W. Fahey, P. M. Forster et al., "Aviation and global climate change in the 21st century," *Atmospheric Environment*, vol. 43, no. 22-23, pp. 3520–3537, 2009.

[4] Deloitte, "Global Aerospace and Defense Industry Outlook," 2014.

[5] D. L. Daggett, R. C. Hendricks, R. Walther, and E. Corporan, "Alternate fuels for use in commercial aircraft," in *Proceedings of the 18th International Symposium on Air Breathing Engines (ISABE '07)*, Beijing, China, 2007.

[6] D. Altiparmak, A. Keskin, A. Koca, and M. Gürü, "Alternative fuel properties of tall oil fatty acid methyl ester-diesel fuel blends," *Bioresource Technology*, vol. 98, no. 2, pp. 241–246, 2007.

[7] M. Canakci, A. N. Ozsezen, E. Arcaklioglu, and A. Erdil, "Prediction of performance and exhaust emissions of a diesel engine fueled with biodiesel produced from waste frying palm oil," *Expert Systems with Applications*, vol. 36, no. 5, pp. 9268–9280, 2009.

[8] P. Arkoudeas, S. Kalligeros, F. Zannikos et al., "Study of using JP-8 aviation fuel and biodiesel in CI engines," *Energy Conversion and Management*, vol. 44, no. 7, pp. 1013–1025, 2003.

[9] B. Gokalp, E. Buyukkaya, and H. S. Soyhan, "Performance and emissions of a diesel tractor engine fueled with marine diesel and soybean methyl ester," *Biomass and Bioenergy*, vol. 35, no. 8, pp. 3575–3583, 2011.

[10] T. Chan, V. Pham, J. Chalmers, C. Davison, W. Chishty, and P. Poitras, "Immediate impacts on particulate and gaseous emissions from a T56 turbo-prop engine using a biofuel blend," SAE Technical Paper 2013-01-2131, 2013.

[11] S. Sumathi, S. P. Chai, and A. R. Mohamed, "Utilization of oil palm as a source of renewable energy in Malaysia," *Renewable and Sustainable Energy Reviews*, vol. 12, no. 9, pp. 2404–2421, 2008.

[12] C. T. Chong and S. Hochgreb, "Spray combustion characteristics of palm biodiesel," in *Proceedings of the 7th Mediterranean Combustion Symposium*, Sardinia, Italy, September 2011.

[13] K. French, "Recycled fuel performance in the SR-30 gas turbine," in *Proceedings of the ASEE Annual Conference and Exposition: Staying in Tune with Engineering Education*, pp. 3651–3656, June 2003.

[14] Z. B. Habib, R. N. Parthasarathy, and S. R. Gollahalli, "Effects of biofuel on the performance and emissions characteristics of a small scale gas turbine," in *Proceedings of the 47th AIAA Aerospace Sciences Meeting including the New Horizons Forum and Aerospace Exposition*, Orlando, Fla, USA, January 2009.

[15] H. W. D. Chiang, I. Chiang, and H. L. Li, "Performance testing of microturbine generator system fueled by biodiesel," in *Proceedings of the ASME Turbo Expo 2007: Power for Land, Sea and Air (GT '07)*, vol. 1, pp. 459–466, ASME, Montreal, Canada, May 2007.

[16] C. R. Krishna, "Performance of the capstone C30 microturbine on biodiesel blends," Tech. Rep., Brookhaven National Laboratory, 2007.

[17] J. Mattingly, *Elements of Propulsion: Gas Turbines and Rockets*, American Institute of Aeronautics and Astronautics, Reston, Va, USA, 2nd edition, 2006.

[18] J. Kurzke, GasTurb 11 Software, 2010.